ized, receptor-channel complexes. The observation that the Hill coefficients for both glycine (Fig. 1C) and NMDA (*10*) are close to 1 is consistent with this interpretation. However, it is not clear yet whether the glycine and glutamate binding sites reside on the same macromolecule, or whether glycine and glutamate influence binding of each other. An alternative mechanism of action of glycine would more closely resemble that of certain enzyme cofactors. In some enzyme systems, for example, a cofactor is required for activation of the enzyme [for example, adenosine 3′,5′-monophosphate (cAMP) for protein kinase A], for binding the substrate in the active site (Mg^{2+} for adenosine triphosphatase), or for creation of the active site (pyridoxal phosphate for transaminases). Regardless of which mechanism of action of glycine proves to be true, it must be able to account for the obligatory nature of glycine for NMDA receptor activation, which is clearly dissimilar to the allosteric modulation of the $GABA_A$ receptor by benzodiazepines.

Second, both glycine and the endogenous agonist, glutamate, are present in the cerebrospinal fluid in micromolar concentrations (*13*). Their presence suggests that the NMDA receptor may be tonically activated, that sensitivity to glycine may be lower in situ, or that some mechanism for "buffering" the glycine and glutamate concentrations at glutamatergic synapses is present. Glutamate uptake systems are at least partially responsible for reducing interstitial glutamate concentration, and uptake systems for glycine have also been described (*14*). If glycine concentration is low in the vicinity of NMDA receptors, a glycinergic synapse could activate NMDA receptors. The receptor could formally be called a "glycine receptor," since both glycine and glutamate are required.

Third, although differences in membrane composition or post-translational processing in oocytes compared to neurons might account for the obligatory nature of glycine in this system, the concentration-response relation for glycine in cultured neurons (*15*) appears very similar to the one presented here. Therefore, our data are likely to represent properties of the native neuronal NMDA receptor.

Finally, because glycine appears to be necessary for NMDA receptor activation, a glycine antagonist or partial agonist might be effective at blocking the pathologies that are associated with intense activation of the NMDA receptor (*16*). More structure-activity studies will facilitate the development of new ligands for the glycine site. Small D–amino acids are effective agonists at the glycine site, which provides a basis for design of additional effective compounds. The oocyte translation system is suitable for these structure-activity studies because it allows precise regulation of drug concentration at the receptor.

REFERENCES AND NOTES

1. D. R. Bristow, N. G. Bowery, G. N. Woodruff, *Eur. J. Pharmacol.* **126**, 303 (1986).
2. J. W. Johnson and P. Ascher, *Nature* **325**, 529 (1987).
3. T. A. Verdoorn, N. W. Kleckner, R. Dingledine, *Science* **238**, 1114 (1987); L. Kushner, J. Lerma, R. S. Zukin, M. V. L. Bennett, *Proc. Natl. Acad. Sci. U.S.A.* **85**, 3250 (1988).
4. I. J. Reynolds, S. N. Murphy, R. J. Miller, *Proc. Natl. Acad. Sci. U.S.A.* **84**, 7744 (1987).
5. D. W. Bonhaus, B. C. Burge, J. O. McNamara, *Eur. J. Pharmacol.* **142**, 489 (1987).
6. E. H. F. Wong, A. R. Knight, R. Ransom, *ibid.*, p. 487.
7. L. D. Snell, R. S. Morter, K. M. Johnson, *Neurosci. Lett.* **83**, 313 (1987).
8. P. R. Schofield *et al.*, *Nature* **328**, 221 (1987).
9. Oocytes were surgically removed from *Xenopus laevis*, rinsed, and placed in a solution of neutral protease (Boehringer Mannheim Biochemicals) (2 mg/ml). After incubation with stirring for about 1 hour, the individual oocytes were placed in 150 m*M* sucrose to shrink the cells, and the follicle cell layer was removed with fine forceps. After injection with 40 to 80 ng of rat brain mRNA (*3*), the oocytes were cultured at 19°C in modified Barth's solution containing 88 m*M* NaCl, 1.0 m*M* KCl, 2.4 m*M* $NaHCO_3$, 10 m*M* Hepes, 0.82 m*M* $MgSO_4$, 0.33 m*M* $Ca(NO_3)_2$, 0.91 m*M* $CaCl_2$, penicillin (0.01 mg/ml), and streptomycin (0.01 mg/ml); pH, 7.3 to 7.4. The cells were cultured for 2 to 5 days before use. The perfusion solution for voltage-clamp experiments was the same as the culture solution, except that the $MgSO_4$ was replaced with $Na_2(SO_4)$, an additional 0.5 m*M* $CaCl_2$ was added, and no antibiotics were included. The water used to make the perfusate was distilled in a closed system in glassware that had been baked at 280°C for 4 hours to destroy glycine. All glassware used in these experiments was treated in this manner unless otherwise indicated. Before such treatment of glassware and solutions, 20 to 50 n*M* glycine was detected in our solutions by high-performance liquid chromatography (HPLC).
10. T. A. Verdoorn and R. Dingledine, *Mol. Pharmacol.*, in press.
11. The dose-response curve (Fig. 1C) is the least squares fit to the logistic equation

$$I_{exp} = \frac{I_{max}}{1 + (EC_{50}/\text{glycine concentration})^n}$$

where n is the Hill slope exponent, I_{exp} is the expected current, and I_{max} is the maximum current. The current expected after perfusion of NMDA in the absence of glycine (I_{min}) was calculated by fitting the data to the equation

$$I_{exp} = \frac{I_{max} - I_{min}}{1 + (EC_{50}/\text{glycine concentration})^n} + I_{min}$$

12. B. Katz and S. Thesleff, *J. Physiol.* **138**, 63 (1957); F. Dreyer, K. Peper, R. Sterz, *ibid.* **281**, 395 (1978); V. E. Dionne, J. H. Steinbach, C. F. Stevens, *ibid.*, p. 421; R. Werman, *Comp. Biochem. Physiol.* **30**, 997 (1969); N. Brooks, M. Blank, R. Werman, *Mol. Pharmacol.* **9**, 580 (1973); N. Brooks and R. Werman, *ibid.*, p. 571.
13. T. N. Ferraro and T. A. Hare, *Brain Res.* **338**, 53 (1985).
14. M. C. Aragon and C. Gimenez, *Biochim Biophys. Acta* **855**, 257 (1986); F. Zafra and C. Gimenez, *Brain Res.* **397**, 108 (1986).
15. J. W. Johnson and P. Ascher, *Soc. Neurosci. Abstr.* **13**, 383 (1987).
16. H. Benveniste, J. Drejer, A. Schousboe, N. H. Diemer, *J. Neurochem.* **43**, 1369 (1984); B. Meldrum, *Clin. Sci.* **68**, 113 (1985); J. Weiss, M. P. Goldberg, D. W. Choi, *Brain Res.* **380**, 186 (1986); S. M. Rothman, J. H. Thurston, R. E. Hauhart, G. D. Clark, J. S. Solomon, *Neuroscience* **21**, 673 (1987); G. D. Clark and S. M. Rothman, *ibid.*, p. 665; R. Gill, A. C. Foster, G. N. Woodruff, *J. Neurosci.* **7**, 3343 (1987); R. Dingledine *et al.*, *CRC Crit. Rev. Neurobiol.*, in press.

17. We thank B. Pallotta, J. McNamara, and R. Miller for helpful comments, and V. Nadler and D. Martin for HPLC measurements of glycine in the solutions. Supported by NIH grants NS23804, NS22249, and NS17771.

7 April 1988; accepted 13 June 1988

Legless, a Novel Mutation Found in PHT1-1 Transgenic Mice

JOHN D. MCNEISH, WILLIAM J. SCOTT, JR., S. STEVEN POTTER

In this report it is shown that the PHT1-1 line of transgenic mice exhibited a pattern of developmental abnormalities when the mice were homozygous for the transgene insertion. Hindlimbs were uniformly truncated at the distal end of the femur, resulting in a "legless" appearance. Forelimbs lacked anterior structures including digits and the radius. The brains had many defects, particularly in the anterior structures of the cerebrum, including the olfactory lobes. Craniofacial malformations in the form of facial clefts also commonly occurred. Furthermore, heterozygotes of this line, with only one copy of the DNA insertion, and other transgenic lines carrying the same DNA construct appeared normal, suggesting that in the PHT1-1 line a gene significant in mammalian development has been disrupted.

IN THE PROCESS OF GENERATING transgenic mice the inserted foreign DNA will sometimes integrate into a host chromosome in a manner that alters an endogenous gene, resulting in a mutation. The potential power of this procedure, referred to as insertional mutagenesis, derives (i) from the production of a mutant mouse,

Division of Basic Science Research and Department of Pediatrics, Children's Hospital Research Foundation and University of Cincinnati College of Medicine, Cincinnati, OH 45229.

allowing the detailed study of the biological impact of altering the gene, and (ii) from the molecular "tagging" of the mutated gene with the inserted foreign DNA sequences, allowing its molecular recovery and analysis (*1, 2*). In particular, Woychik *et al.* (*3*) have isolated a mouse line with the transgene interrupting a mouse gene of some developmental consequence. Mice homozygous for the transgene (and hence the interruption) exhibit abnormal limbs, with the ulna fused to the radius and the tibia fused to the fibula. Here we report the description of a new transgenic mouse line in which heterozygotes, with one normal chromosome and one carrying the transgene, appeared normal, but homozygotes exhibited numerous abnormalities.

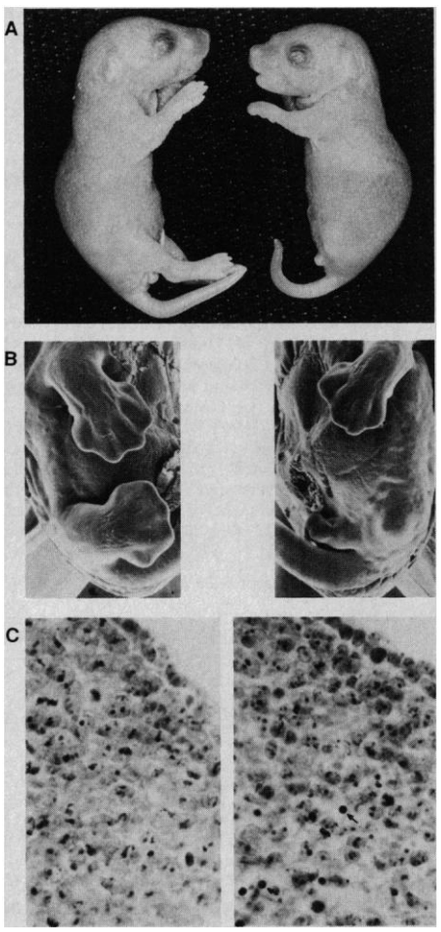

Fig. 1. The legless mutation phenotype in newborn mice and embryos. (**A**) Wild-type (left) and legless (right) newborn mice were littermates resulting from mating of heterozygous PHT1-1 transgenic mice. The mutant demonstrates characteristic loss of hindlimb structures, aberrant forelimbs with ectrodactyly of preaxial digits, and a small bump on the cranium, which signals brain abnormality. (**B**) Scanning electron micrograph (SEM) of limbs in a wild-type (left) and legless mutant embryo (right) at day 12 of gestation. The mutant hindlimb demonstrates arrested development. (**C**) Histologic sections from hindlimb buds of day 10 wild-type embryos (left) and mutant embryos (right). Abnormal cell death in mutant limb buds is indicated by pycnotic nuclei (arrows).

Transgenic mice were produced by injecting into zygotes a DNA construct made by Pelham (*4*), that carries a *Drosophila* heat shock gene (*hsp70*) and a herpesvirus thymidine kinase gene. *Drosophila hsp70* sequences can serve as a useful inducible promoter in mouse tissue culture cells (*5*). Three independent original (F_0) transgenic mice were born carrying this DNA construct, and all were of normal phenotype. However, when we interbred the transgenic progeny of one of these mice, designated PHT1-1, approximately 25% of the newborn pups exhibited the mutant phenotype shown in Fig. 1A. From 16 matings terminated before parturition, 118 progeny were collected of which 30 exhibited the mutant phenotype. Yet when PHT1-1 heterozygotes were mated to nontransgenic siblings there were no mutant progeny. These observations are compatible with the presence of an autosomal recessive insertional mutation caused by the transgene. In addition, direct DNA hybridization analysis with the transgene sequence probe has shown that mutant mice were invariably homozygous for the transgene insertion, whereas normal phenotype mice were heterozygous or nontransgenic (Fig. 2). A total of 60 mutant mice and embryos have now been confirmed as homozygotes in this manner. Hybridization intensities, as compared to copy control lanes loaded with known amounts of linearized pHT1 plasmid DNA, suggested a concatemer size of 20 to 30 copies, with mutants having twice this amount. This finding strongly suggests that the mutation is recessive and is caused by the transgene disruption of an endogenous gene that plays an important role in development. A less likely explanation is that there is an extremely sensitive dose-response threshold and that although a single copy of the transgene concatemer gives perfectly normal mice, two copies of the added concatemer and its products result in the unusual mutant phenotype observed.

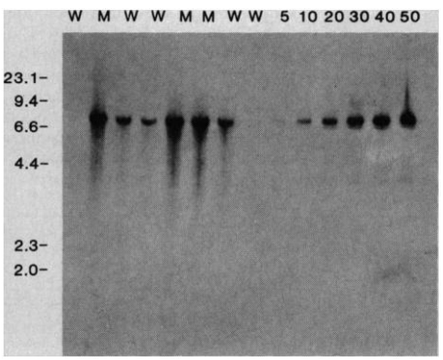

Fig. 2. Molecular analysis of the genotypes of newborn mice from matings of heterozygous PHT1-1 transgenics. Genomic DNA (2.0 μg) digested with Bam HI and separated by electrophoresis on a 0.7% agarose gel. Gel contains genomic DNA from eight offspring of PHT1-1 heterozygous matings and copy controls to determine size of transgene concatemer accurately. DNA was assayed ($R^2 > 0.99$ for standards) fluorometrically as described (*11*). DNA blot was hybridized to a labeled probe of linearized pHT1 plasmid DNA. The mutant phenotype (M) cosegregates with the homozygous genotype for the transgene pHT1. Two wild-type (W) mice are nontransgenic with no hybridization signal, and three are heterozygotes with a concatemer size of 20 to 30 copies per haploid genome. DNA was transferred to GeneScreen Plus, hybridized at 65°C, and washed according to manufacturer's procedures. Linearized pHT1 probe DNA was labeled with [^{32}P] adenosine triphosphate by the random primer method (*12*). Size markers consisting of λ DNA digested by Hind III are shown, in kilobases, on the left.

Seventy-two newborn mutant mice have been analyzed by a combination of procedures including razor blade sectioning (*6*), skeletal staining (*7*), and dissection. The most striking aspect of the newborn mutant phenotype was the loss of most visible hindlimb structures (Fig. 1A). In the mutant the hindlimbs are reduced to mere stubs. To

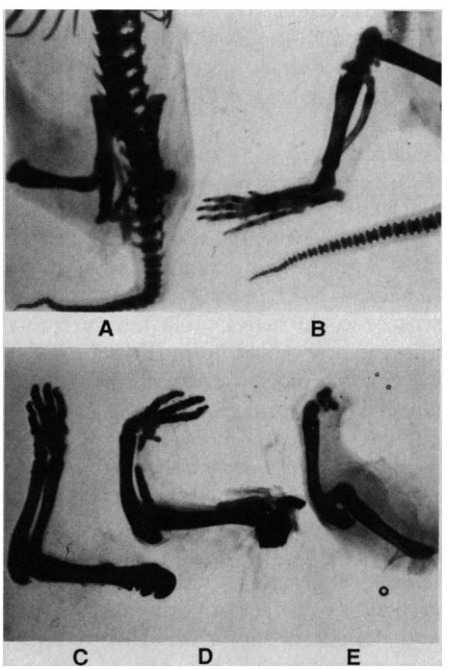

Fig. 3. Skeletal analysis of hindlimbs and forelimbs from the legless mutation. (**A**) Skeletal staining of hindlimb from a legless mutant. (**B**) Hindlimb of a control mouse. (**C, D,** and **E**) Analysis of three dissected forelimbs from legless mutants, demonstrating the preaxial manifestation of the mutation. (C) Ectrodactyly 1 only. (D) Ectrodactyly 1 and 2 with rudimentary radius. (E) Nearly complete loss of all digits and the carpus, and total loss of the radius. Cartilage was stained with Alcian blue, and the bone was stained with Alizarine Red S by a modified method described by Kimmel and Trammell (*7*).

determine the embryological origins of this malformation, we examined the early stages of the mutant hindlimb development. Figure 1B shows that at day 12 of gestation the hindlimbs are already much smaller than normal. At day 11, the mutant hindlimbs are still much reduced. At day 10 the wild-type and mutant hindlimbs are quite similar in size and structure; however, histological sections reveal the occurrence of abnormal mesenchymal cell death in the mutants (Fig. 1C). This cell death first appears in the anterior portion of the hindlimb bud and may play a causal role in the generation of the malformed hindlimb observed in the newborn. The skeletal composition of normal newborn mouse hindlimbs and those of the legless mutant were also compared (Fig. 3, A and B). More than 90% of newborn mutants had hindlimbs that included a complete femur but lacked further distal development. One newborn had a rudimentary femur in the left hindlimb, and one newborn had some trivial skeletal development distal to the femur.

The forelimbs were also almost always (142 out of 144) abnormal, but in contrast to the hindlimbs, a great diversity of expression was the rule. The least severe expression seen was absence of digit one; the most severe, the loss of the radius and all structures distal to the carpus. This loss of skeletal elements from the autopod and zeugopod occurred with a definite predilection for preaxial (anterior) structures (Fig. 3, C to E), suggesting that the interrupted gene has important functions in pattern formation during normal limb development.

Craniofacial malformations were another prominent feature of the mutant phenotype. Cleft lip or cleft palate, or both, occurred with moderate frequency (40%). Moreover, all mutants examined (26) had brain anomalies. Manifestations included highly aberrant or missing olfactory lobes in almost all mutants, and many had hemorrhagic protrusions from the cerebral cortex (Fig. 4A), which could be seen externally as bumps located between the eyes in 46% of newborns. Other irregularities in newborn brains included hydrocephalus of the lateral ventricles, thinning of the nasal septum, and abnormal brain shape. Significant brain abnormalities were also observed at very early stages of development. For example, in the 20-somite embryo the anterior (cranial) portion of the neuroepithelium showed cell disorganization and necrosis (Fig. 4B).

This pattern of malformations has not to our knowledge been seen in other mouse mutants. The hindlimb malformation is rarely seen in mammalian offspring from any cause, genetic or chemical. There is, however, a similarity to a few avian mutants. Abbot (*8*) described "stumpy" in turkeys as a semidominant gene in which rear limb development of homozygotes is usually restricted to a femur. Hinchliffe and Ede (*9*) described a wingless chick mutant in which the forelimbs are usually absent and the hindlimbs are reduced by the absence of preaxial digits and the tibia, the preaxial bone in the leg. The hindlimb of wingless chick mutants and the forelimb of legless transgenic mice thus share the same pattern of missing skeletal elements, and our initial observations suggest that the cause of skeletal loss, necrosis of limb anterior mesenchyme cells, is the same in both mutants.

An additional observation was the shortened life expectancy of homozygous legless newborns. None has yet survived for 24 hours after birth even though another study (*10*) indicated that nearly all homozygotes were alive just before parturition. Death was thus a postnatal phenomenon, but the cause remains unknown.

In conclusion, the transgene in the PHT1-1 line of mice appears to have disrupted an endogenous gene that normally plays an important role in limb and craniofacial development. Further embryological analysis of the mutants will generate information regarding the developmental defects and the molecular mechanism. Moreover, retrieval of flanking sequences, identification of evolutionarily conserved regions, and direct molecular analysis of the gene and its products should now be possible.

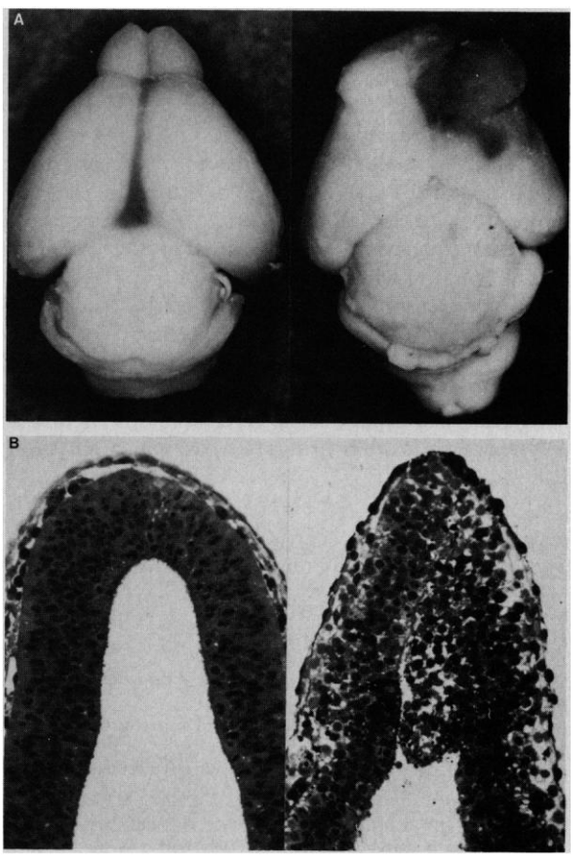

Fig. 4. Brain dysmorphology in the legless mutation. (**A**) The dissected brains from a wild-type newborn mouse (left) and from a legless mutant newborn mouse (right). Structures readily identifiable in the control, anterior to posterior (top to bottom), are the olfactory lobes, cerebral hemispheres, mesencephalon, and cerebellum. In the legless mutant the loss of the olfactory lobes, a large hemorrhagic protrusion of the right cerebral hemisphere, a smaller protrusion of the left cerebral hemisphere, and the loss of distinction between hemispheres of the cerebrum can be observed. (**B**) Histologic sections of the developing brains of 20-somite wild-type embryo (left) and legless mutant (right) embryo. The magnification (×50) of the anterior (cranial) neural tube in the control embryo demonstrates a well-developed, highly organized neuroepithelium with many characteristic mitotic figures at the internal surface. The mutant embryo histology demonstrates neuroepithelial disorganization and cell death with necrotic cell debris infiltrating the neural canal. Embryo genotypes are determined by genomic DNA extraction from the yolk sac of the conceptus and by DNA blotting as described in the legend to Fig. 2.

REFERENCES AND NOTES

1. R. D. Palmiter and R. L. Brinster, *Annu. Rev. Genet.* **20**, 465 (1986); T. Gridley, P. Soriano, R. Jaenisch, *Trends Genet.* **3**, 162 (1987).
2. R. Jaenisch *et al.*, *Cell* **32**, 209 (1983); P. Soriano *et al.*, *Genes Div.* **1**, 366 (1987); L. Covarrubias *et al.*, *Cold Spring Harbor Symp. Quant. Biol.* **50**, 447 (1985); W. H. Mark, K. Signorelli, E. Lacy, *ibid.*, p. 453; M. Shani, *Mol. Cell. Biol.* **6**, 2624 (1986); R. D. Palmiter *et al.*, *Cell* **36**, 869 (1984); P. A. Overbeek *et al.*, *Science* **231**, 1574 (1986).
3. R. P. Woychik *et al. Nature* **318**, 36 (1985).
4. H. R. B. Pelham, *Cell* **30**, 517 (1982).
5. F. M. Wurm, K. A. Gwinn, R. E. Kingston, *Proc. Natl. Acad. Sci. U.S.A.* **83**, 5414 (1986).
6. J. G. Wilson, in *Teratology: Principles and Techniques*, J. G. Wilson and J. Warkany, Eds. (Univ. of Chicago Press, Chicago, 1965), pp. 251–261.
7. C. A. Kimmel and C. Trammell, *Stain Technol.* **56**, 271 (1981).
8. U. Abbot, in *Limb Development and Regeneration*, J. Fallon and A. Caplan, Eds. (Liss, New York, 1983), part A, pp. 13–31.
9. J. R. Hinchliffe and D. A. Ede, *J. Embryol. Exp. Morphol.* **30**, 753 (1973).
10. J. D. McNeish *et al.*, unpublished data.
11. C. Labarca and K. Paigen, *Anal. Biochem.* **102**, 344 (1980).
12. A. P. Feinberg and B. Vogelstein, *ibid.* **132**, 6 (1983).

13. We thank F. Constantini for teaching us how to make transgenic mice and C. Schreiner for technical assistance. K. Sulik and J. Thayer provided the micrograph of developing neuroepithelium and H.-J. Merker the SEM of day 12 mouse embryos. Supported by grants from the National Cancer Institute, NIH, and the Amoco Foundation.

22 March 1988; accepted 10 June 1988